Available online at www.sciencedirect.com
SCIENCE DIRECT®
International Journal of Pharmaceutics 280 (2004) 17–26
international journal of pharmaceutics
www.elsevier.com/locate/ijpharm

Crystal structure and surface properties of an investigational drug—A case study☆

Y.-H. Kiang[a,*], H. Galen Shi[a,*], David J. Mathre[b], Wei Xu[a], Dina Zhang[c], Santipharp Panmai[a]

[a] *Pharmaceutical Research and Development, Merck Research Laboratories, Merck and Co. Inc., P.O. Box 4, West Point, PA 19426, USA*
[b] *Process Research, Merck Research Laboratories, Merck and Co., Inc., 126 E. Lincoln Avenue, Rahway, NJ 07065, USA*
[c] *Pharmaceutical Research and Development, Merck Research Laboratories, Merck and Co. Inc., 126 E. Lincoln Avenue, Rahway, NJ 07065, USA*

Received 11 February 2004; received in revised form 15 April 2004; accepted 15 April 2004

Abstract

In this study we investigate the correlations between the single crystal structure, the crystal habitat and morphology, and surface energetics of an investigational pharmaceutical compound. Crystal structure of this investigational pharmaceutical solid has been solved from single crystal X-ray analysis. Crystallographic data are as follows: triclinic, *P*1 (no. 1), $a = 6.1511\ (8)$ Å, $b = 13.5004\ (18)$ Å, $c = 17.417\ (2)$ Å, $\alpha = 68.259\ (2)^\circ$, $\beta = 80.188\ (2)^\circ$, $\gamma = 82.472\ (2)^\circ$, $V = 1320.2\ (3)$ Å^3, $Z = 2$. The external morphology of this crystalline solid was predicted by molecular modelling using attachment energies to be thin-plate like with a dominant face (0 0 1). The predicted morphology was confirmed by scanning electron micrographs (SEM) and the Miller Index of the dominant face was complemented by X-ray powder diffraction (XRPD) method. The microscopic layering structures of crystals and surface stability of the dominant faces were investigated using atomic force microscopy (AFM). Contact angle measurement showed that the surface of the dominant face is hydrophilic as predicted from crystal structure.
Published by Elsevier B.V.

Keywords: Morphology prediction; Single crystal structure; Attachment energies; Surface structures; Atomic force microscopy

1. Introduction

The majority of active pharmaceutical ingredients used in solid dosage formulations are crystalline solids. An individual crystal exhibits a number of crystal faces, each with its own physical and chemical properties. When the pharmaceutical crystals shows a few dominant faces that contribute to most of the crystal surface area, the physical and chemical properties of those faces are important as they transport to the bulk properties including wettability, dissolution rate, flowability and tablettability (York et al., 1998; Muster and Prestidge, 2002; Buller et al., 2002; Chen et al., 2002).

Knowledge of the surface structure at the atomic level is the first step towards understanding of the physical and chemical properties of the crystal faces. In order to determine the surface structure of a

☆ Supplementary data associated with this article can be found at doi:10.1016/j.ijpharm.2004.04.022.

* Corresponding authors.
E-mail addresses: yuanhon_kiang@merck.com (Y.-H. Kiang), galen_shi@merck.com (H.G. Shi).

0378-5173/$ – see front matter Published by Elsevier B.V.
doi:10.1016/j.ijpharm.2004.04.022

particular crystal face, one needs to obtain both the crystal structure and the Miller index of that particular crystal face. Crystal structures of small molecules can be determined from either single crystal or powder X-ray diffraction methods. The Miller indices of the prominent faces of a large single crystal can be indexed directly using X-ray diffraction or reflecting Goniometer. For microcrystallites, indexing the Miller indices is more challenging as the crystals are too small to be mounted on a Goniometer head. Nonetheless, several methods have been developed and reported for indexing Miller indices of microcrystallites using scanning electron micrographs (SEM) in conjunction with computer programs based on geometric procedures (Strom, 1976; Simov et al., 1983). Computer programs developed for morphology prediction based on single crystal structures can also be used to determine Miller indices provided the morphology is calculated correctly. The calculated morphology must be examined experimentally to assure the validity of the morphology simulation. Scanning electron microscopy is often used to compare the observed and calculated morphology. The dominant faces can also be examined by the powder X-ray diffraction method (Jenkins and de Veris, 1997; Morris et al., 2000).

Atomic force microscopy (AFM) has become a powerful tool to study the surface microstructure, morphology and adhesion properties of pharmaceutical crystals. Drug crystal surfaces were imaged with AFM to monitor the crystal face-specific dissolution in situ where the intrinsic dissolution rate could be calculated for particular crystal planes (Danesh et al., 2001). The milled drug crystals were also imaged with AFM and large contrast in the phase images was observed on the milled drug surfaces, which were attributed to amorphous regions induced by milling (Begat et al., 2003). A recent paper described the application of AFM in imaging crystalline drug nanoparticles deposited from a dispersion or embedded in a solid dosage form for their particle size determination (Shi et al., 2003). AFM was used to study the interaction forces between drug crystal faces and hydrophobic or hydrophilic colloidal AFM probes, and the adhesion forces were found to be correlated with the surface energies from contact angle measurement and the surface chemistry data from the time-of-flight secondary ion mass spectrometry (ToF-SIMS) (Muster and Prestidge, 2002). In another study to probe the mechanism of tablet sticking to punch faces of the tablet press, iron coated AFM probes were used to measure the work of adhesion between iron and profen compounds. The AFM results of the rank order of drugs in sticking tendency were in agreement with that predicted by molecular simulation (Wang et al., 2003).

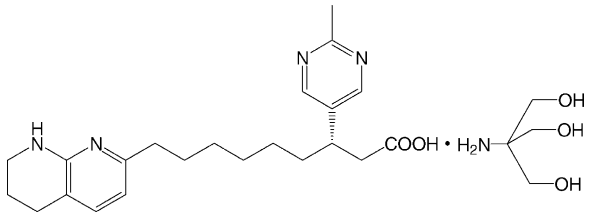

Scheme 1.

In this study we investigate the correlations between the single crystal structure, the crystal habitat and morphology, and surface energetics of an investigational drug 1·Tris (Scheme 1). The morphology of 1·Tris was calculated using the attachment energy method. The calculated morphology was then validated using microscopic method and the Miller index of the dominant face was examined using X-ray diffraction method. The crystal surface structure and the wettability of the dominant face were investigated using AFM and contact angle measurement, respectively. This work shows a corroborative study on drug crystal structures and surface properties using theoretical calculation and experimental measurements.

2. Theory

The simulated morphology was the growth morphology based on the attachment energy method (Docherty et al., 1991). The attachment energy (E_{att}) is defined as the energy released on the attachment of a growth slice to a growing surface Eq. (1). In Eq. (1), E_{latt} is the lattice energy of the crystal and E_{sl} is the slice energy, which is defined as the energy of a growth slice of thickness *dhkl*.

$$E_{att} = E_{latt} - E_{sl} \quad (1)$$

The attachment energy is calculated on suitable slices (*hkl*), which are usually chosen by performing a

geometric prediction of the possible growth faces (Bravais Friedel Donnay Harker method). The growth rate of a crystal face is proportional to its attachment energy. The faces with the lowest attachment energies are slowest growing and, hence, have the morphological dominance, i.e. the largest surface exposure (Berkovitch-Yellin, 1985).

3. Experimental section

Compound 1·Tris (3(*S*)-(2-methyl-pyrimidin-5-yl)-9-(5,6,7,8-tetrahydro-[1,8]naphthyridin-2-yl)nonanoic acid tris(hydroxymethyl)aminomethane salt) used in this study was prepared at Merck & Co., Inc. with greater than 98% purity. All analytical grade solvents were purchased from Aldrich and used without further purification. Compound 1·Tris (10 mg, 0.02 mmol) was dissolved with 6 mL of a 1:1 mixture of methanol and nitromethane in a clean vial. This solution was then moved to a fume-hood, where slow evaporation of the solvent yielded thin plate-shaped single crystals suitable for X-ray data collection after 5 days.

Single crystal X-ray data were collected on a Siemens Smart diffractometer equipped with a CCD area detector using Mo Kα radiation. Diffraction data were collected at 298 K. All structure solutions were obtained with a direct method and refined using full-matrix least squares, on the basis of F_0^2, with Shelxl 97. All atomic parameters were independently refined. A summary of parameters for the X-ray data collection and subsequent refinement is given in Table 1. The non-hydrogen atoms were refined anisotropically. Hydrogen atoms were included in the last stage of the refinement at their geometrically constrained positions. Tables of bond distances, bond angles, and anisotropic thermal factors appear in the supplement. Powder X-ray diffraction data were recorded on a Philips PW3040-PRO X-ray diffractometer equipped with a multiplewire detector at 40 kV, 40 mA for Cu Kα.

The computation was performed on an SGI Octane workstation with a R12000 processor at 400 MHz. The morphology simulation and analysis were performed using *Morphology*, which is integrated in the simulation package *Cerius*^{2}.

The thin plate-shaped crystals were placed on a clean glass coverslide and examined with an AFM (Dimension 3100 SPM, Digital Instruments). The dominant faces and edges of thin plates were focused for AFM imaging with the aid of a built-in optical lens. The AFM instrument was operated in air at 20 °C in the tapping mode with a TESP etched silicon probe (Digital Instruments). Height images were collected and analyzed with the Nanoscope III software (Digital Instruments).

The drug crystals were examined using an environmental SEM Quanta 200 (FEI Co.) in a low vacuum mode. The electron accelerating voltage was 20 kV and the water vapor pressure was 0.76 Torr. In the contact angle measurement, a powder compact was made from crystal particles using a Carver Press (Carver Inc.) at a pressure of 10,000 psi and a drop of a testing liquid (water) was placed onto the drug compact. The images of the liquid were collected using a video based contact angle goniometer (Future Digital Scientific Inc.). The first stable image was used to extract the contact angle.

Table 1
Crystal data and refinement for 1·Tris

Formula	$C_{26}H_{41}N_5O_5$
Formula weight	503.64
T (K)	298 (2)
Wavelength (Å)	0.71073
Crystal system	Triclinic
Space group	$P1$
a (Å)	6.1514 (9)
b (Å)	13.5003 (19)
c (Å)	17.416 (2)
α (°)	68.257 (2)
β (°)	80.191 (2)
γ (°)	82.473 (2)
V (Å^3)	1320.2 (3)
Z	2
ρ_{calc} (g/cm^3)	1.267
Absorption coefficient (mm^{-1})	0.089
θ range for data collection (°)	1.27–26.39
Limiting indices	$-7 \le h \le 7$, $-16 \le k \le 16$, $-21 \le l \le 21$
No. of data/restrains/parameters	5365/7/659
No. of reflection collected/unique reflections	14094/5365
Absorption correction	None
Goodness-of-fit on F^2	1.069
$R1$[a]	0.0740 ($I > 2\sigma(I)$)
w$R2$[a]	0.2100 ($I > 2\sigma(I)$)

[a] $R1 = \Sigma \, ||F_c| - |F_0|| / |F_c|$, $wR2 = \Sigma[w(F_0^2 - F_c^2)]^2 / \Sigma[w(F_0^2)^2]]^{1/2}$.

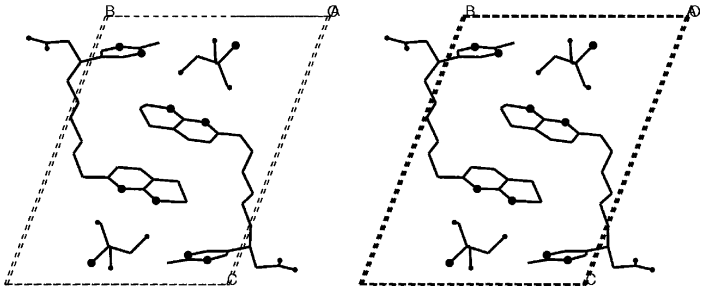

Fig. 1. Stereoview of crystal structure of 1·Tris viewed down the *a* axis. Hydrogen atoms are removed for clarity.

4. Results and discussion

4.1. Single crystal structure

As shown in Scheme 1, there are multiple hydrogen-bonding donor and acceptor groups in 1·Tris to form an extensive hydrogen-bonding network. Specifically molecule 1 has a carboxylic acid group, an amino group and a pyridinium nitrogen atom as hydrogen-bonding donors and acceptors and its counter-ion, tris molecule, also has hydrogen-bonding donors and acceptors in its three hydroxy groups and one amino group. Molecule 1 has a chiral center at the carbon where the methyl pyrimidine group is attached. The bulk 1·Tris is optically pure; therefore it is only allowed to crystallize in chiral space groups. The single crystal structure of 1·Tris is illustrated in Fig. 1. As one sees in Fig. 1, two crystallographically non-equivalent 1 molecules and two tris salts are arranged in a pseudo-centrosymmetric pairing. Viewing down the *a* axis, one sees that one 1 molecule is shaped as a horse shoe with the opening facing

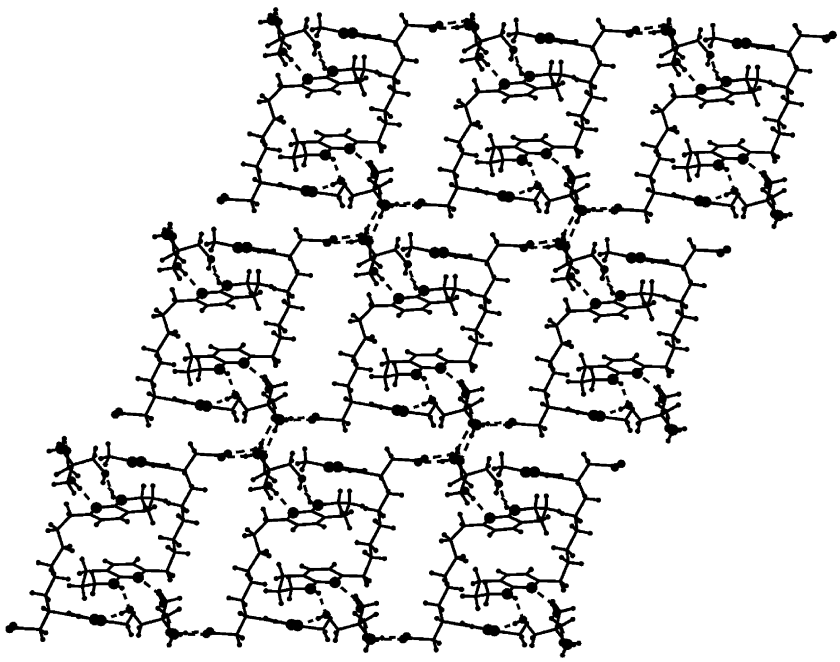

Fig. 2. Two-dimensional hydrogen-bonded network of 1·Tris. Nitrogen: large sphere; oxygen: medium sphere; hydrogen: small sphere; carbon: stick; hydrogen bonding: dashed line.

to the right and the other 1 molecule forms another horse shoe with the opening facing to the left. These two 1 molecules, if viewed down the *a* axis, seem to interlock into each other to form a train-coupler-like unit; however, viewing down the *b* axis, the two 1 molecules are actually away from each other by half an unit cell along the *a* axis. The "train coupler" units are hydrogen-bonded through tris molecules into a two-dimensional network along the *a* and *b* directions. Fig. 2 shows this two-dimensional network. In Fig. 2, one sees that along the horizontal direction there is a chain composed of molecule 1 and tris alternately while vertically two tris moieties are stacked together with one molecule 1 above and another beneath. These two-dimensional layers are stacked along the *c* axis and connected through the tris moieties into a three-dimensional hydrogen-bonded network.

4.2. Crystal morphology calculation

The dominant face and the morphology of 1·Tris were calculated using the attachment energy method. It is essential to a successful attachment energy calculation that a proper force field is used. In the case of 1·Tris, the crystal structure is based on a three-dimensional hydrogen bonding network. The force field "Drieding 2.21" (Mayo et al., 1990) was chosen as it accounts for hydrogen bonds explicitly (Payne et al., 1998). The electrostatics potential (ESP) of the molecule is assigned by the charge equilibration (Q_{eq}) method (Rappe and Goddard, 1991). The single crystal structure of 1·Tris was energetically minimized using the force field "Drieding 2.21" in conjunction with Ewald summation with the cell dimensions and atomic coordinates free to relax. The minimized structure was compared to the single crystal structure. The similarity between the crystal structures before and after minimization indicates that the "Drieding 2.21" is suitable for energy calculation of this hydrogen-bonded crystal system.

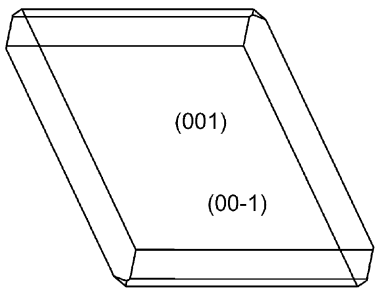

Fig. 3. Calculated morphology of 1·Tris showing dominant faces (0 0 1) and (00-1).

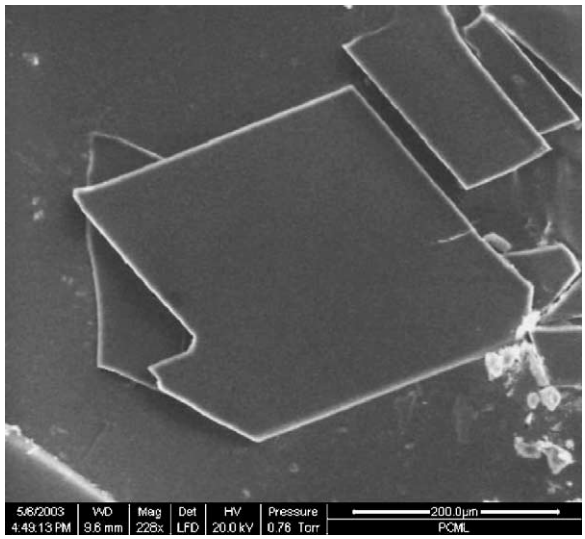

Fig. 4. Scanning electron micrograph of several 1·Tris crystals showing the dominant face.

The minimized crystal structure of 1·Tris was used to calculate the crystal morphology. "Dreiding 2.21" was again used as the force field while the Ewald summation was replaced by Direct summation because the current Morphology module does not support Ewald summation for evaluating van der Waals interactions. Using the attachment energy method, the morphology

Table 2
Attachment and slice energies calculated of observed faces of 1·Tris

h	*k*	*l*	E_{att} (kJ/mol)	E_{sl} (kJ/mol)
0	0	1	−12.77	−175.13
0	0	−1	−12.77	−175.13
1	1	0	−49.88	−138.02
−1	−1	0	−49.88	−138.02
−1	−2	−2	−74.04	−113.16
1	2	2	−74.04	−113.16
0	−1	−1	−76.81	−111.09
0	1	1	−76.81	−111.09
0	1	0	−78.11	−109.79
0	−1	0	−78.11	−109.79
−1	0	0	−96.10	−91.80
1	0	0	−96.10	−91.80

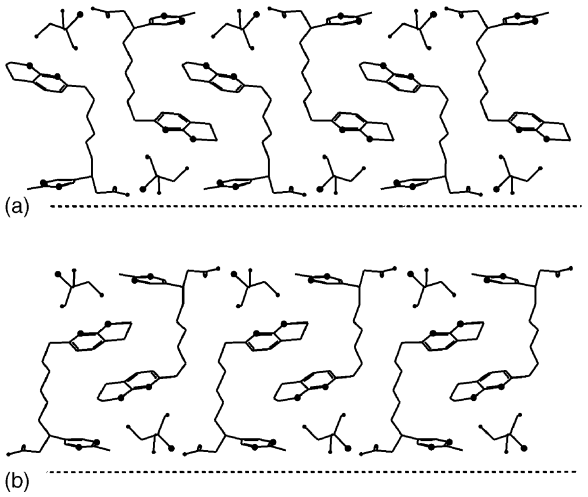

Fig. 5. Surface structure of (a) (0 0 1) and (b) (00-1) faces of 1·Tris showing a depth of 16.01 Å (1 unit cell). Nitrogen: large sphere; oxygen: small sphere; hydrogen atoms are removed for clarity.

of 1·Tris was calculated as a thin plate, illustrated in Fig. 3. The observed morphology of 1·Tris from scanning electron microscopy is shown in Fig. 4. A comparison of the morphology predicted by calculation to that from the scanning electron micrograph shows a good similarity in crystal shape and crystal faces, indicating the calculated result is reasonably accurate.

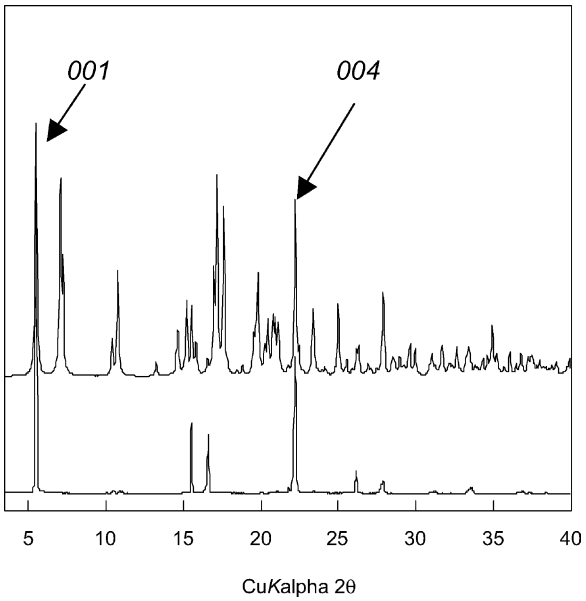

Fig. 6. X-ray diffraction patterns of 1·Tris calculated from single crystal structure (top) and observed from large crystals with the dominant faces exposed to radiation (bottom).

4.3. Surface functional groups and wettability

The calculated attachment energy of the observed faces is listed in Table 2. The lowest attachment

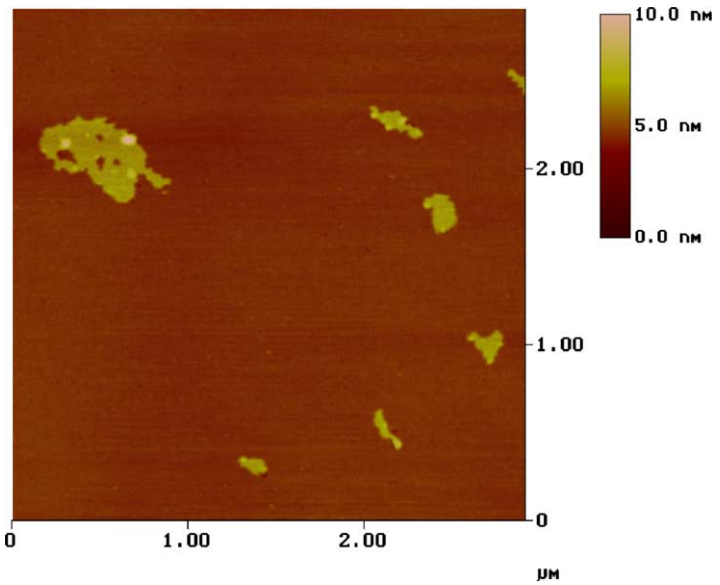

Fig. 7. Tapping mode AFM picture (scan size: 3 μm × 3 μm) of a typical area on the surface of a thin plate drug crystal.

energy is −12.77 kcal/mol for both the faces (0 0 1) and (00–1). The faces (0 0 1) and (00–1) are therefore the most dominant faces. The surface structures of the dominant faces (0 0 1) and (00–1) are illustrated in Fig. 5. As the 1·Tris is packed around a pseudo inversion center, the resulting molecular arrangement on face (0 0 1) and (00–1) should be identical. Indeed, in Fig. 5, the surface structures of the two dominant faces are identical as the carboxylate and tris groups are exposed to the surface. The contact angle of compound 1·Tris with water was found to be 19° ± 5°, indicating a rather hydrophilic surface, which is in agreement with the surface exposure of carboxylate and tris groups as expected.

4.4. X-ray diffractometric studies

The dominant faces of 1·Tris were examined using X-ray diffraction. Large plate-shaped crystals of 1·Tris were carefully placed on a channel-cut silicon zero-background sample holder in such a way that the dominant faces of 1·Tris are coplanar with the sample holder surface. Both the observed and the calculated XRPD patterns of compound 1·Tris are shown in Fig. 6. As one sees in Fig. 6, there is a significant discrepancy in peak intensities between the calculated and observed XRPD patterns due to the effect of preferred orientation. In the observed powder pattern, the two most intense peaks are 0 0 1 and 0 0 4 reflections. Because both these intense reflections belong

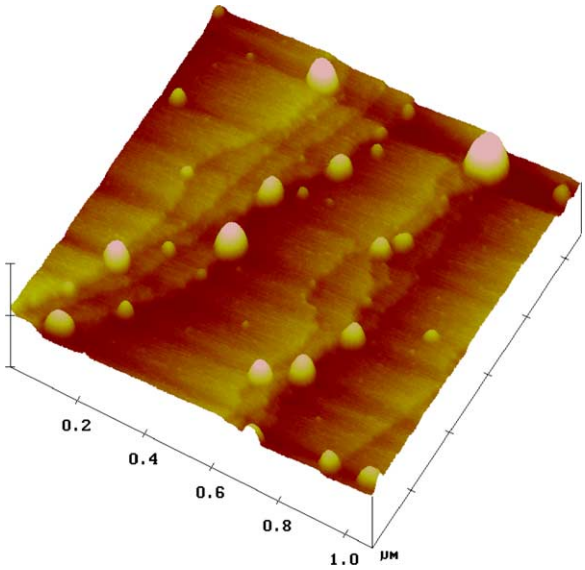

Fig. 9. Three-dimensional AFM image of the edge area of a thin plate crystal.

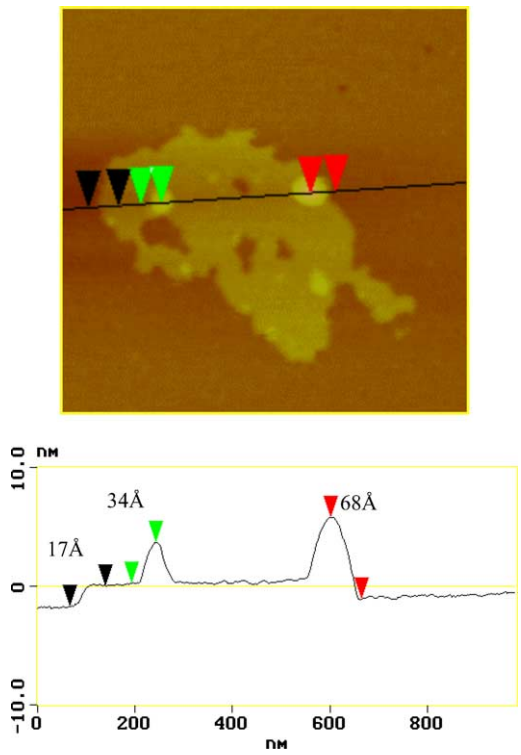

Fig. 8. Cross section analysis of an enlarged area in Fig. 7.

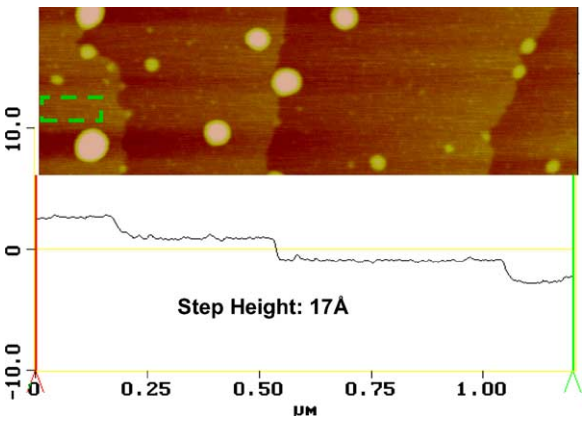

Fig. 10. Cross section analysis of an enlarged area in Fig. 9.

to {0 0 1}, surface (0 0 1) is indeed the dominant face of this thin-plate crystal.

4.5. AFM studies

AFM imaging of the dominant face of thin plate crystals revealed microscopic layering structures and provided experimental confirmation of crystal lattice dimensions derived from single crystal X-ray diffraction. Fig. 7 shows a typical picture where several molecular islands of sub-microns in lateral dimensions sit on an atomically smooth surface. The enlarged image of the large island and its cross section profile in Fig. 8 indicate that the island is composed of one base layer of molecules with a few stacked add-on layers and several delaminated areas, since the distances between the layers were measured to be the integer numbers of 17 Å (e.g., 17, 34 and 68 Å), which

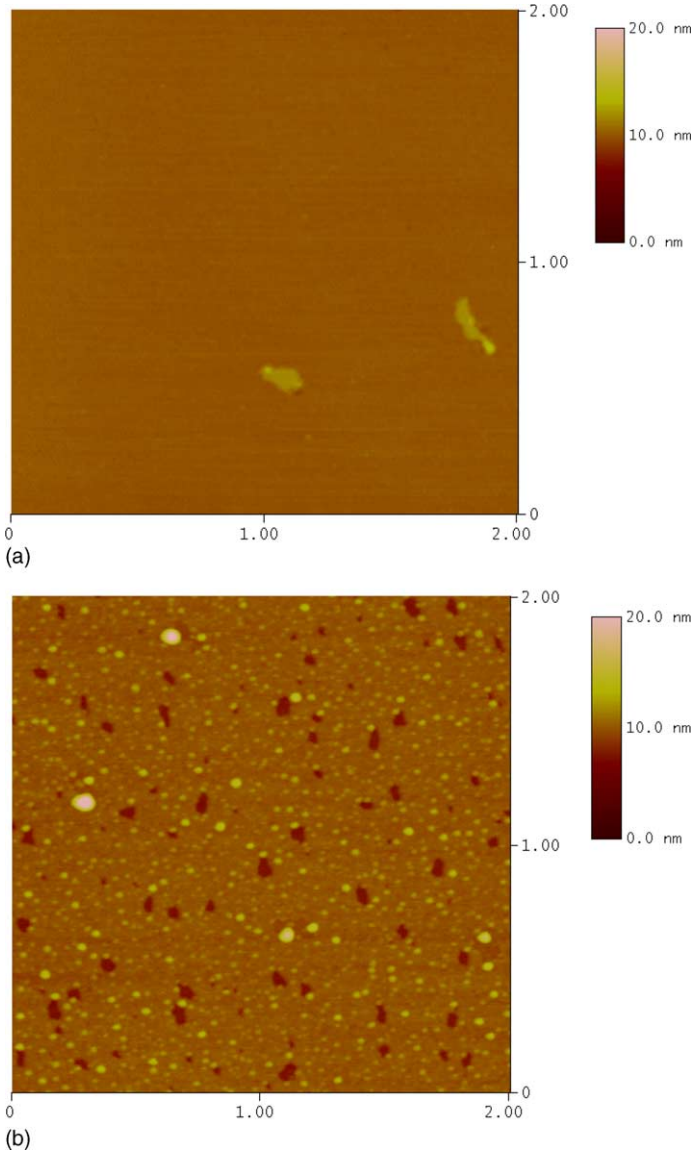

Fig. 11. AFM images of crystal (0 0 1) plane before (a) and after (b) exposure to 20 °C/40% RH for 24 h.

agrees reasonably well with the *d*-spacing of 16 Å between (0 0 1) planes determined by single crystal diffraction.

When the edge areas of thin plate crystals were examined, a terraced structure with stacked molecular clusters was resolved as shown in Fig. 9. The terraces are formed by single crystal planes growing layer upon layer, because the crystal step height was measured to be 17 Å, as shown in Fig. 10. The small islands are probably the isolated molecular layers in a three-dimensional manner, i.e. growing vertically as well as laterally, despite the prevalent crystal growth in a two-dimensional or lateral expansion mode along the (0 0 1) plane.

The surface stability of the (0 0 1) plane was also monitored by AFM. After exposing the crystal to the laboratory environment (20 °C/40% RH) for 24 h, the originally smooth (0 0 1) plane with some add-on layers became very different in microstructure. Layers were found missing in many locations and new islands were growing in the meantime. Overall, the surface roughness for the 2 μm × 2 μm areas in Fig. 11 has increased significantly from 0.173 nm in R_q (root mean square roughness) to 0.749 nm. It is possible that the water layer adsorbed on the crystal surface facilitated this simultaneous drug dissolution and recrystallization. Such a change in crystal surface morphology may have an impact to formulation processing and drug dissolution.

5. Conclusions

The concept of using molecular modelling to predict the crystal morphology and to determine the surface structure of particular faces of a crystal has been successfully applied to an investigational pharmaceutical solid. The surface structure and properties predicted from molecular modelling were corroborated by AFM and contact angle measurement.

Acknowledgements

The authors wish to thank Dr. Richard Ball for valuable discussions and Ms. Nancy Tsou for assistance with recrystallization work to obtain X-ray quality single crystals of 1·Tris.

References

Begat, P., Young, P.M., Edge, S., Kaerger, J.S., Price, R., 2003. The effect of mechanical processing on surface stability of pharmaceutical powders: visualization by atomic force microscopy. J. Pharm. Sci. 92, 611–620.

Buller, R., Peterson, M.L., Almarsson, Ö., Leiserowitz, L., 2002. Quinoline binding site on malaria pigment crystal: a rational pathway for antimalaria drug design. Crystal Growth Design 2, 553–562.

Berkovitch-Yellin, Z., 1985. Toward an ab initio derivation of crystal morphology. J. Am. Chem. Soc. 107, 8239–8253.

Chen, X., Morris, K.R., Grieeser, U.J., Byrn, S.R., Stowell, J.G., 2002. Reactivity difference of indomethacin solid forms with ammonia gas. J. Am. Chem. Soc. 124, 15012–15019.

Danesh, A., Connell, S.D., Davies, M.C., Roberts, C.J., Tendler, S.J.B., Williams, P.M., Wilkins, M.J., 2001. An in situ dissolution study of asprin crystal planes (1 0 0) and (0 0 1) by atomic force microscopy. Pharm. Res. 18, 299–303.

Docherty, R., Clydesdale, G., Roberts, K.J., Bennema, P., 1991. Application of Bravais–Fredel–Donnay–Harker, attachment energy and lsing models to predicting and understanding the morphology of molecular crystals. J. Phys. D: Appl. Phys. 24, 89–99.

Jenkins R., de Veris J.L., 1997. An Introduction to Powder Diffractometry. Philips, Eindhoven, The Netherlands.

Mayo, S.L., Olafson, B.D., Goddard III, W.A., 1990. DREIDING: a generic force field for molecular simulations. J. Phys. Chem. 94, 8897–8909.

Morris, K.R., Schlam, R.F., Cao, W., Short, M.S., 2000. Determination of average crystalline shape by X-ray diffraction and computational methods. J. Pharm. Sci. 89, 1432–1442.

Muster, T.H., Prestidge, C.A., 2002. Face specific properties of pharmaceutical crystals. J. Pharm. Chem. 91, 1432–1444.

Muster, T.H., Prestidge, C.A., 2002. Application of time-dependent sessile drop contact angles on compacts to characterise the surface energetics of sulfathiazole crystals. Int. J. Pharm. 234, 43–54.

Payne, R.S., Roberts, R.J., Rowe, R.C., Docherty, R., 1998. Generation of crystal structures of acetic acid and its halogenated analogs. J. Comput. Chem. 19, 1–20.

Rappe, A.K., Goddard Jr., W.A., 1991. Charge equilibration for molecular dynamics simulations. J. Phy. Chem. 95, 3358–3363.

Shi, H.G., Farber, L., Michaels, J.N., Dickey, A., Thompson, K.C., Shelukar, S.D., Hurter, P.N., Reynolds, S.D., Kaufman, M.J., 2003. Characterization of crystalline drug nanoparticles using atomic force microscopy and complementary techniques. Pharm. Res. 20, 479–484.

Simov, S., Simova, E., Davidkov, B., Mechenov, G., 1983. A geometric method incorporated with a computer program for indexing crystal faces of microcrystallites. J. Appl. Cryst. 16, 559–562.

Strom, C.S., 1976. Indexing crystal faces on SEM photographs. J. Appl. Cryst. 9, 291–295.

Wang, J.J., Li, T., Bateman, S.D., Erck, R., Morris, K.R., 2003. Modeling of adhesion in tablet compression. Part I. Atomic force microscopy and molecular simulation. J. Pharm. Sci. 92, 798–814.

York, P., Ticehurst, M.D., Osborn, J.C., Robert, R.J., Rowe, R.C., 1998. Characterisation of the surface energetics of milled dl-propranolol hydrochloride using inverse gas chromatography and molecular modelling. Int. J. Pharm. 174, 179–186.